

## Magnetic susceptibility of cerium: An LDA+DMFT study

S. V. Streltsov,<sup>1,2</sup> E. Gull,<sup>3</sup> A. O. Shorikov,<sup>1,2</sup> M. Troyer,<sup>4</sup> V. I. Anisimov,<sup>1,2</sup> and P. Werner<sup>5,4</sup>

<sup>1</sup>*Institute of Metal Physics, S. Kovalevskoy St. 18, 620041 Ekaterinburg GSP-170, Russia*

<sup>2</sup>*Ural Federal University, Mira St. 19, 620002 Ekaterinburg, Russia\**

<sup>3</sup>*Department of Physics, Columbia University, New York, 10027, USA*

<sup>4</sup>*Theoretical Physics, ETH Zurich, 8093 Zurich, Switzerland*

<sup>5</sup>*Department of Physics, University of Fribourg, 1700 Fribourg, Switzerland*

The magnetic properties of Ce in the  $\alpha$  and  $\gamma$  phase are calculated within the local-density approximation and dynamical mean-field theory (LDA+DMFT) approach. The magnetic susceptibility in these two phases shows a similar behavior over a wide temperature range: a Curie-Weiss law at high temperatures, indicating the presence of local moments, followed by a maximum in a crossover regime, and a saturation characteristic of a state with screened local moments at low temperature. The difference in experimentally observable magnetic properties is caused by the shift of the susceptibility to higher temperatures in the  $\alpha$  phase compared to the  $\gamma$  phase.

### I. INTRODUCTION

The isostructural  $\alpha - \gamma$  transition in Ce is one of the classical problems in modern solid-state physics. In the low-temperature  $\alpha$  phase (up to  $T \sim 100$  K at normal conditions, or up to  $T \sim 300$  K for a pressure  $P$  of 1 GPa), Ce behaves like a Pauli paramagnet, while in the high-temperature  $\gamma$  phase the susceptibility approximately follows a Curie-Weiss law.<sup>1</sup> The transition is accompanied by a drastic volume collapse (9%–15%)<sup>1</sup> and dramatic changes of the electronic spectra.<sup>2</sup>

A number of theoretical models were proposed to describe the  $\alpha - \gamma$  transition. One of the first was a promotional model, where localized  $4f$  electrons were suggested to transfer to the  $spd$ -(valence) band state, losing their local moments.<sup>3,4</sup> This was in contradiction to later experimental results that showed that the number of  $4f$  electrons is almost unchanged during the transition.<sup>5</sup> As a result, a Mott-like picture was proposed, where the valence of the Ce ions does not change, but the transition, which affects the degree of  $4f$  electron localization, occurs as a result of the change of the ratio of on-site  $f - f$  Coulomb interaction ( $U$ ) to kinetic energy.<sup>6</sup>

Further neutron experiments<sup>7</sup> confirmed that the Ce- $4f$  electrons remain localized and indicated that the Kondo volume collapse model<sup>8,9</sup> could be more plausible. According to this model, the  $4f$  electrons remain localized in the low-temperature  $\alpha$  phase but form Kondo singlets with conduction electrons in the  $spd$  band. As a result of this strong coupling, the local spin moments of the  $4f$  electrons get screened, which leads to the volume collapse in the Kondo regime. Thus a full account of the hybridization between localized  $4f$  and band  $spd$  electrons is needed for the correct description of Ce. Moreover, it was recently shown that  $f - f$  hopping is also important and should be taken into consideration.<sup>10</sup>

Full information about the noninteracting band structure of Ce can be obtained within the framework of the density-functional theory (DFT), e.g., in the local-density approximation (LDA). These density-functional calculations can be extended to include local correlations within the LDA+DMFT scheme (combination of local-density approximation and dynamical mean-field theory).<sup>11</sup>

“*Ab initio*” calculations in the LDA+DMFT approach were successfully applied to the modeling of electronic and structural properties of Ce. They have illustrated the key role of the entropic contribution to the free energy<sup>12,13</sup> and the importance of the formation of a quasiparticle peak<sup>14,15</sup> for the description of the  $\alpha - \gamma$  transition in Ce. The applicability of the Kondo model was mainly discussed via an analysis of the spectral properties of the two phases: the temperature dependence of the quasiparticle resonance<sup>15,16</sup> or features of the Ce- $spd$  bands.<sup>17</sup> Meanwhile, the description of a key physical observable, namely, the temperature dependence of magnetic susceptibility (for which different models were originally proposed), has not yet been attempted.

In the present report we use the LDA+DMFT method to calculate the magnetic properties of Ce in the  $\alpha$  and  $\gamma$  phases. The results of the study show that the temperature dependence of the magnetic susceptibility is very similar in Ce- $\alpha$  and Ce- $\gamma$ , and that both phases should thus be described by the same model. The difference in the observed magnetic properties is attributed to the decrease of the hybridization between localized  $f$  and conductive  $spd$  electrons, which leads to a shift of the magnetic susceptibility curve to lower temperatures in Ce- $\gamma$ .

### II. CALCULATION DETAILS

We performed LDA calculations using the linearized muffin-tin orbitals (LMTO) method.<sup>18</sup> An almost orthogonalized version of the LMTO in the  $\Gamma$  representation with Ce  $6s$ ,  $6p$ ,  $5d$ , and  $4f$  states included to the basis set was used. The Hamiltonian was generated on a mesh of 1728  $k$  points in the full Brillouin zone (BZ). This LDA Hamiltonian was then transformed to a basis set with a diagonal form at the  $\Gamma$  point. In this basis set the three lowest energy states at the  $\Gamma$  point correspond to the  $t_{1u}$ , the next three to the  $t_{2u}$ , and the highest energy states to the  $a_{2u}$  irreducible representation.

The on-site Coulomb repulsion parameter ( $U$ ) was estimated to be 6.0 eV using a constrained supercell calculation. This is in agreement with previous results.<sup>19</sup> The intra-atomic Hund’s rule coupling was set to  $J_H = 0$  eV.

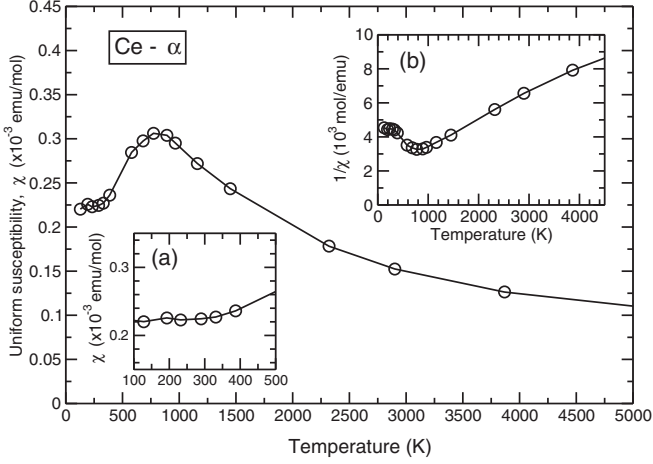


FIG. 1. Uniform magnetic susceptibility  $\chi(T)$  for Ce- $\alpha$ . Inset (a): enlarged view of  $\chi(T)$  in the low-temperature region. Inset (b): inverse magnetic uniform susceptibility  $\chi^{-1}(T)$ .

For the solution of the DMFT equations we employed a diagrammatic (“continuous-time CT-HYB”) quantum Monte Carlo algorithm which samples the partition function in powers of the impurity-bath hybridization.<sup>20,21</sup> The Coulomb term was treated in the density-density form. The double counting correction was set to  $E_{dc} = U(n_{\text{DMFT}} - \frac{1}{2})$ ,<sup>11</sup> with  $n_{\text{DMFT}}$  the total number of  $4f$  electrons self-consistently obtained within DMFT. The LDA+DMFT calculations were not fully self-consistent in the sense that the LDA charge density was not recalculated after the DMFT run. This can be done since the total number of the  $4f$  electrons does not change significantly. The Ce  $4f$  spectral functions were calculated using the maximum entropy method.<sup>22</sup> We first computed the self-energy  $\Sigma$  on the real frequency axis and used it to obtain the orbitally resolved and total spectral functions.

We calculated the uniform magnetic susceptibility  $\chi$  as the ratio of the field-induced magnetization change  $dm(T)$  and the energy change  $\delta E$  associated with the applied field ( $h$ ):

$$\chi = \left. \frac{dm}{dh} \right|_{h \rightarrow 0} = \frac{n_{\uparrow} - n_{\downarrow}}{\delta E} \mu_B^2. \quad (1)$$

Here  $n_{\uparrow}$  and  $n_{\downarrow}$  are the total occupation numbers for spin up and down. The susceptibility  $\chi$  was calculated for  $\delta E = 0.01$  eV, which is within the interval where  $m(T)$  is a linear function of  $\delta E$ .

### III. RESULTS

The uniform magnetic susceptibility  $\chi(T)$  for the Ce- $\alpha$  phase, obtained using the LDA+DMFT calculations, is shown in Fig. 1. In the low-temperature region the magnetic susceptibility is temperature independent up to  $\sim 300$  K. This is in qualitative agreement with experimental findings.<sup>23</sup> The absolute value of the magnetic susceptibility is underestimated in LDA+DMFT by comparison with  $\chi$  measured for  $P = 1$  GPa, where the presence of the structurally different Ce- $\beta$  phase is minimal. The experimental value of  $\chi$  is  $\sim 0.6\text{--}0.7 \times 10^{-3}$  emu/mol, while the theoretical estimate is  $0.22 \times 10^{-3}$  emu/mol. The underestimation of the magnetic susceptibility could be due to the absence of long-range correlations in our single-site DMFT calculations. Also, the

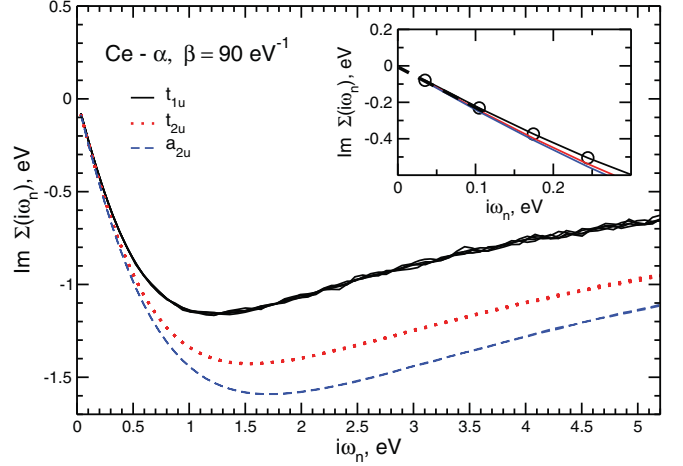


FIG. 2. (Color online) Imaginary part of the self-energy for all 14  $4f$  orbitals at  $T = 129$  K ( $\beta = 90$  eV $^{-1}$ ) in Ce- $\alpha$ . Due to the crystal-field splitting, they form three different sets of curves denoted as  $t_{1u}$ ,  $t_{2u}$ , and  $a_{2u}$ . The inset shows the low-energy behavior of  $\text{Im}\Sigma(i\omega_n)$ . For one of the curves, exact positions of Matsubara frequencies and linear extrapolation (dashed line) to zero are shown.

spin-orbit coupling and associated orbital moment are not captured within our simple LDA description.

The plateau in the susceptibility of Ce at low temperatures corresponds to a coherent regime, where all  $4f$  electrons with local moments are screened. Indeed, one may notice from Fig. 2 that in this temperature region the imaginary part of the self-energy for all  $4f$  orbitals is linear and approaches zero for low Matsubara frequencies. This is a signature that the system at these temperatures is in a coherent Fermi-liquid regime.

The importance of the screening effects by  $spd$  electrons is most clearly seen when one compares Fig. 1, inset (a), and Fig. 3. The local magnetic susceptibility presented in Fig. 3 was calculated as

$$\chi_0 = \int_0^\beta \langle S_z(\tau) S_z(0) \rangle d\tau, \quad (2)$$

where  $\beta$  is the inverse temperature, and  $\langle S_z(\tau) S_z(0) \rangle$  is the imaginary time-dependent spin-spin correlation function.

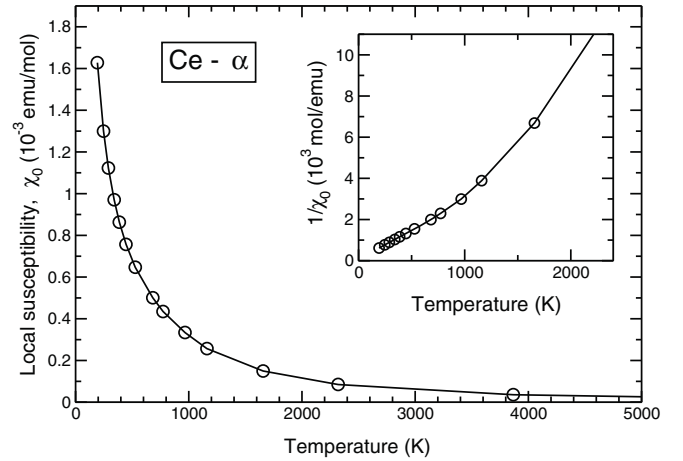


FIG. 3. Local magnetic susceptibility  $\chi_0(T)$  and inverse local magnetic susceptibility  $\chi_0^{-1}(T)$  for Ce- $\alpha$ .

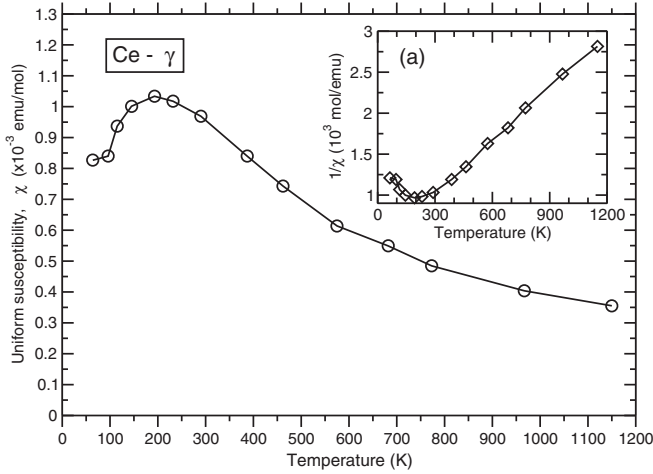


FIG. 4. Uniform magnetic susceptibility  $\chi(T)$  and inverse magnetic uniform susceptibility  $\chi^{-1}(T)$  for Ce- $\gamma$ , inset (a).

In spite of the strong nonlinearity of the inverse uniform susceptibility, the local susceptibility follows a  $\chi_0^{-1}(T) = T/C$  law up to  $T \approx 1000$  K. This implies that the  $4f$  electrons retain the local nature of the magnetic moment, even at very low temperatures, and there is no delocalization process. The violation of the Curie-Weiss law of uniform susceptibility [Fig. 1, inset (b)] and coherence of the system [which is seen in Fig. 2] is caused by the screening of local spins by conduction electrons.

With increasing temperature the screening effects weaken. This leads to an increase of the entropy according to Ref. 12. Note that the growth of the susceptibility starts at  $\sim 350$  K, i.e., in the region where the  $\alpha - \gamma$  transition occurs.

At temperatures above 350 K, the experimentally stable phase of Ce is the  $\gamma$ , not the  $\alpha$  phase. However, we may still simulate the magnetic properties of Ce- $\alpha$ , even in a temperature region where it does not exist by using the LDA band structure of the corresponding phase. In making such calculations one concludes that the temperature range  $350 \text{ K} < T < 1000 \text{ K}$  is a crossover region where the system can neither be described as a coherent electron liquid nor as a lattice of localized  $f$  states weakly hybridized to conduction electrons. The maximum in the uniform magnetic susceptibility at 820 K appears as a result of a competition between Kondo and local spin regimes. Interestingly, in the Coqblin-Schrieffer model this maximum appears if the degeneracy of the impurity level is more than 3.<sup>24,25</sup> This is in agreement with the present results, where the degeneracy of the lowest energy  $t_{1u}$  states equals 6 (for both spins).

A behavior consistent with the Curie-Weiss law,  $1/\chi(T) \sim T$ , for the uniform susceptibility is only seen above 1000 K [Fig. 1, inset (a)].

The uniform magnetic susceptibility in the  $\gamma$  phase [Fig. 4] is qualitatively similar to the one just described for Ce- $\alpha$ . With Curie-Weiss-like behavior at high temperature, a crossover region characterized by a maximum in the susceptibility, followed by a drastic drop and (at the lowest accessible temperatures) a saturation. The difference is mainly in the numbers. Already at  $T = 300$  K, the uniform magnetic susceptibility of Ce in the  $\gamma$  phase is Curie-Weiss like. The

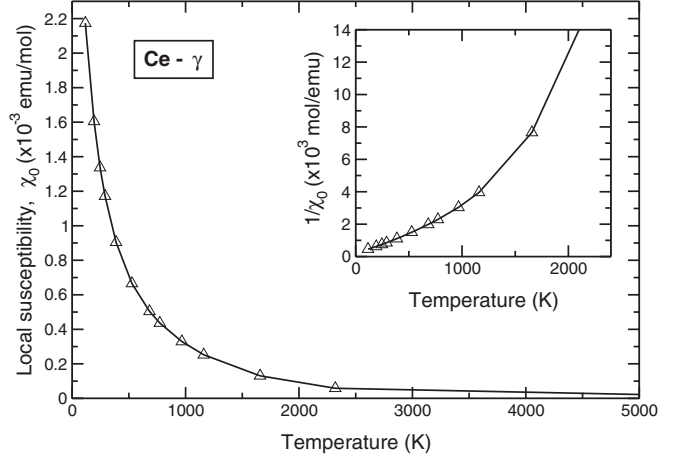


FIG. 5. Local magnetic susceptibility  $\chi_0(T)$  and inverse magnetic local susceptibility  $\chi_0^{-1}(T)$  for Ce- $\gamma$ .

broad maximum marking the crossover region is at  $\sim 200$  K, much lower than in Ce- $\alpha$ . However, since the  $\gamma$  phase experimentally exists only above 300 K, the crossover regime and the constant  $\chi(T)$  regime found below  $\sim 90$  K are not accessible in measurements.

The absolute value of the calculated  $\chi$  in the region around 500 K, where it is experimentally measurable, is underestimated (as in the  $\alpha$  phase). We find  $\sim 0.7 \times 10^{-3}$  emu/mol while the experimental value is  $\sim 1.4 \times 10^{-3}$  emu/mol.<sup>23</sup> As one may see in Fig. 5, the local magnetic susceptibility  $\chi_0$  for Ce- $\gamma$  is similar to that for Ce- $\alpha$  and follows a  $C/T$  law up to  $T < 1000$  K. At higher temperatures  $\chi_0^{-1}$  shows a deviation from the linear behavior with an upturn of the curve. A similar upturn can be observed for the inverse susceptibility of the one-band Hubbard model in the correlated metal regime ( $U = 2.5$ ,  $W = 2$ ).<sup>26</sup> This effect is due to the fact that at higher temperatures the thermal fluctuations become so large that the spins at different  $\tau$  points become uncorrelated and “do not feel” each other, i.e., that  $\langle S_z(\tau)S_z(0) \rangle \sim C \rightarrow 0$  with  $T \rightarrow \infty$ . The result is a deviation of the local susceptibility  $\chi_0^{-1} = T/C(T)$  from the Curie law.

#### IV. DISCUSSION

The shape of the susceptibility curves for the  $\alpha$  and  $\gamma$  phases is very similar. Moreover, it strongly resembles  $\chi(T)$  obtained in models with a projected Hilbert space, such as the Coqblin-Schrieffer impurity,<sup>24,25</sup> its lattice version,<sup>27</sup> and also  $\chi(T)$  in the periodic Anderson model.<sup>28</sup> The uniform static magnetic susceptibility in all these models is characterized by a high-temperature Curie-Weiss tail, a maximum in the intermediate regime, and then a drastic drop with a constant susceptibility at the lowest temperatures.

The high-temperature behavior of  $\chi(T)$  is explained by the presence of local moments and described in a similar manner in all of the models, while the drastic decrease of the magnetic susceptibility at intermediate temperatures is caused by the screening of this moment. The lattice effects such as nonzero hopping between localized and conductive states, centered at different sites, are already taken into account in our LDA+DMFT calculation. The results clearly show

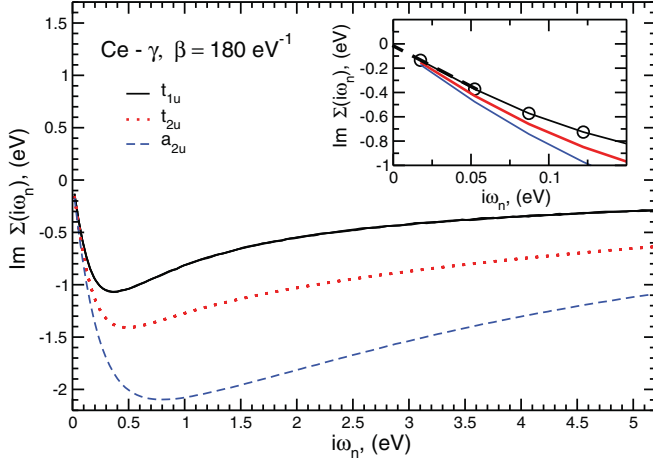


FIG. 6. (Color online) Imaginary part of the self-energy for all 14  $4f$  orbitals at  $T = 64$  K in Ce- $\gamma$ . Due to the crystal-field splitting, they form three different sets of curves denoted as  $t_{1u}$ ,  $t_{2u}$ , and  $a_{2u}$ . The inset shows the low-energy behavior of  $\text{Im}\Sigma(i\omega_n)$ . For one of the curves, exact positions of Matsubara frequencies and linear extrapolation (dashed line) to zero are shown.

the formation of a coherent state with  $\text{Im}\Sigma(i\omega_n) \rightarrow 0$  at low temperatures (see Figs. 2 and 6). Meanwhile, an inspection of the spectral functions, plotted in Fig. 7, shows that there is no gap or pseudogap in the vicinity of the Fermi level in the  $f$ -electron spectral function. Note that here we present results at considerably lower temperatures than in previous DMFT studies.

Comparing Figs. 1 and 4, one sees that the behavior of the uniform magnetic susceptibility in  $\alpha$ -Ce and  $\gamma$ -Ce is qualitatively the same. The susceptibility in the  $\gamma$  phase seems to be shifted to the low-temperature region and renormalized (as compared with Ce- $\alpha$ ). Thus, one may argue that those phases are physically similar in a wide temperature range.

The change of the lattice volume under the  $\alpha - \gamma$  transition results in a modification of the hybridization function in the vicinity of the Fermi level and a decrease of the  $f - f$  hopping. The weakening of the hybridization in Ce- $\gamma$  (see Ref. 16, for instance) leads to a decrease of the exchange parameter  $J_K$  in the Kondo model according to the Schrieffer-Wolff transformation.<sup>29</sup> Numerical calculations show that the decrease of the Kondo exchange results in a shift of the maximum of the magnetic susceptibility to lower temperatures.<sup>25</sup> This is exactly what is seen in Ce under the  $\alpha - \gamma$  transition. A similar shift of the maximum of  $\chi(T)$  due to a change of the hybridization was also observed in the study of the magnetic properties of the periodic Andersen model.<sup>28</sup>

It is also instructive to compare the present results with the situation in Pu, which is on the border of the transition between the actinide elements with localized and delocalized electrons.<sup>30</sup> Moreover, the degree of localization changes in the different phases of Pu.<sup>31,32</sup> The DMFT calculations of Pu show that the local magnetic susceptibility dramatically changes from Pauli-like to Curie-Weiss as the volume increases.<sup>33</sup> This is completely different from the situation observed in Ce, where the local susceptibility follows a  $1/T$  law for both the  $\alpha$  and  $\gamma$  phases. This is further evidence for the absence

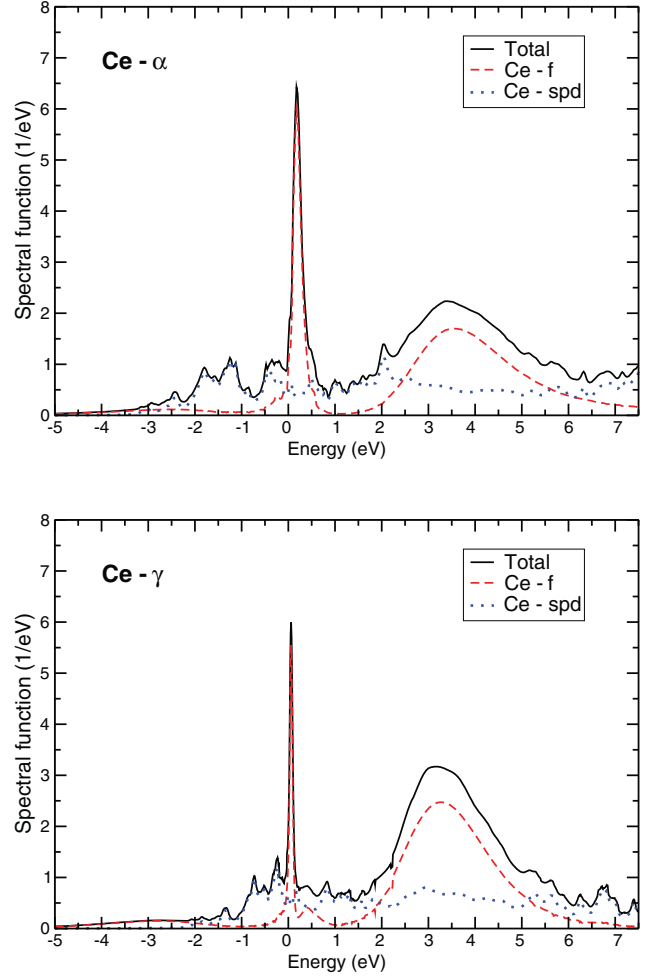


FIG. 7. (Color online) Top panel: spectral function for the Ce- $\alpha$  phase calculated for  $\beta = 90 \text{ eV}^{-1} \sim 130$  K. Bottom panel: spectral function for the Ce- $\gamma$  phase calculated for  $\beta = 180 \text{ eV}^{-1} \sim 65$  K.

of any localization/delocalization transitions in the  $4f$  shell of Ce, i.e., against the Mott transition scenario.

To summarize, in the present paper the magnetic susceptibility for the  $\alpha$  and  $\gamma$  phases of Ce was investigated. It exhibits a qualitatively similar behavior in both phases. There is no Mott transition for any of the Ce phases. On the local level they are both characterized by the presence of magnetic moments, screened by band  $spd$  electrons at low temperatures. With increase of the temperature this coherent state with constant susceptibility is gradually destroyed by thermal excitations, which results in the formation of a Curie-Weiss paramagnetic state in the high-temperature region. The difference in experimentally observable magnetic properties for the two phases of Ce is related to a shift of the susceptibility in Ce- $\gamma$  to the lower temperature region (as compared to  $\alpha$  phase).

## ACKNOWLEDGMENTS

We thank S. Skornyakov and A. Poteryaev for help with the calculations of the local susceptibilities. This work was supported by Grants No. RFBR 10-02-00046 and No. 10-02-96011, the program of the President of the Russian Federation



MK-309.2009.2, a grant from the Ural Branch of the Russian Academy of Science for Young Scientists, SNF Grant No.

PP0022-118866 and NSF-DMR-1006282. The calculations were based on the ALPS (Ref. 34) DMFT (Ref. 35) package.

\*streltsov@imp.uran.ru

- <sup>1</sup>D. Koskenmaki and K. A. Gschneidner, *Handbook on the Physics and Chemistry of Rare Earths* (Elsevier, Amsterdam, 1978), Chap. 4.
- <sup>2</sup>L. Z. Liu, J. W. Allen, O. Gunnarsson, N. E. Christensen, and O. K. Andersen, *Phys. Rev. B* **45**, 8934 (1992).
- <sup>3</sup>A. F. Schuch and J. H. Sturdivant, *J. Chem. Phys.* **18**, 145 (1950).
- <sup>4</sup>A. Lawson and T. Tang, *Phys. Rev.* **76**, 301 (1949).
- <sup>5</sup>D. Gustafson, J. McNutt, and L. Roellig, *Phys. Rev.* **183**, 435 (1969).
- <sup>6</sup>B. Johansson, *Philos. Mag.* **30**, 469 (1974).
- <sup>7</sup>A. P. Murani, S. J. Levett, and J. W. Taylor, *Phys. Rev. Lett.* **95**, 256403 (2005).
- <sup>8</sup>J. W. Allen and R. M. Martin, *Phys. Rev. Lett.* **49**, 1106 (1982).
- <sup>9</sup>M. Lavagna, C. Lacroix, and M. Cyrot, *Phys. Lett. A* **90**, 210 (1982).
- <sup>10</sup>S. V. Streltsov, A. O. Shorikov, and V. I. Anisimov, *JETP Lett.* **92**, 543 (2010).
- <sup>11</sup>V. I. Anisimov, A. I. Poteryaev, M. A. Korotin, A. O. Anokhin, and G. Kotliar, *J. Phys.: Condens. Matter* **9**, 7359 (1997).
- <sup>12</sup>B. Amadon, S. Biermann, A. Georges, and F. Aryasetiawan, *Phys. Rev. Lett.* **96**, 066402 (2006).
- <sup>13</sup>L. de' Medici, A. Georges, G. Kotliar, and S. Biermann, *Phys. Rev. Lett.* **95**, 066402 (2005).
- <sup>14</sup>K. Held, A. K. McMahan, and R. T. Scalettar, *Phys. Rev. Lett.* **87**, 276404 (2001).
- <sup>15</sup>A. K. McMahan, K. Held, and R. T. Scalettar, *Phys. Rev. B* **67**, 075108 (2003).
- <sup>16</sup>M. B. Zöfl, I. A. Nekrasov, T. Pruschke, V. I. Anisimov, and J. Keller, *Phys. Rev. Lett.* **87**, 276403 (2001).
- <sup>17</sup>K. Haule, V. Oudovenko, S. Y. Savrasov, and G. Kotliar, *Phys. Rev. Lett.* **94**, 036401 (2005).
- <sup>18</sup>O. K. Andersen and O. Jepsen, *Phys. Rev. Lett.* **53**, 2571 (1984).
- <sup>19</sup>V. I. Anisimov and O. Gunnarsson, *Phys. Rev. B* **43**, 7570 (1991).
- <sup>20</sup>P. Werner, A. Comanac, L. de' Medici, M. Troyer, and A. J. Millis, *Phys. Rev. Lett.* **97**, 076405 (2006).
- <sup>21</sup>E. Gull, A. J. Millis, A. I. Lichtenstein, A. N. Rubtsov, M. Troyer, and P. Werner, *Rev. Mod. Phys.* **83**, 349 (2011).
- <sup>22</sup>R. N. Silver, D. S. Sivia, and J. E. Gubernatis, *Phys. Rev. B* **41**, 2380 (1990).
- <sup>23</sup>T. Naka, T. Matsumo, and N. Mori, *Physica B* **205**, 121 (1995).
- <sup>24</sup>V. T. Rajan, *Phys. Rev. Lett.* **51**, 308 (1983).
- <sup>25</sup>J. Otsuki, H. Kusunose, P. Werner, and Y. Kuramoto, *J. Phys. Soc. Jpn.* **76**, 114707 (2007).
- <sup>26</sup>S. Streltsov, S. Skornyakov, A. Poteryaev, and V. Anisimov (unpublished).
- <sup>27</sup>J. Otsuki, H. Kusunose, and Y. Kuramoto, *J. Phys. Soc. Jpn.* **78**, 034719 (2009).
- <sup>28</sup>H. J. Leder and G. Czyczoll, *Z. Phys. B* **35**, 7 (1979).
- <sup>29</sup>J. Schrieffer and P. Wolff, *Phys. Rev.* **149**, 491 (1966).
- <sup>30</sup>K. T. Moore and G. v. d. Laan, *Rev. Mod. Phys.* **81**, 235 (2009).
- <sup>31</sup>N. Baclet, M. Dorneval, L. Havela, J. M. Fournier, C. Valot, F. Wastin, T. Gouder, E. Colineau, C. T. Walker, S. Bremier *et al.*, *Phys. Rev. B* **75**, 035101 (2007).
- <sup>32</sup>L. Havela, T. Gouder, F. Wastin, and J. Rebizant, *Phys. Rev. B* **65**, 235118 (2002).
- <sup>33</sup>C. A. Marianetti, K. Haule, G. Kotliar, and M. J. Fluss, *Phys. Rev. Lett.* **101**, 056403 (2008).
- <sup>34</sup>B. Bauer *et al.*, *J. Stat. Mech.* (2011) P05001.
- <sup>35</sup>E. Gull, P. Werner, S. Fuchs, B. Surer, T. Pruschke, and M. Troyer, *Comput. Phys. Commun.* **182**, 1078 (2011).